Polyhedron xxx (2014) xxx–xxx

Contents lists available at ScienceDirect

Polyhedron

journal homepage: www.elsevier.com/locate/poly

Dual investigation of lanthanide complexes with cinnamate and phenylacetate ligands: Study of the cytotoxic properties and the catalytic oxidation of styrene

Alberto Aragón-Muriel [a], María Camprubí-Robles [b], Elena González-Rey [b], Alfonso Salinas-Castillo [c], Antonio Rodríguez-Diéguez [d], Santiago Gómez-Ruiz [e,*], Dorian Polo-Cerón [a,*]

[a] Departamento de Química, Universidad del Valle, Calle 13 No 100-00, Cali 76001000, Colombia
[b] Institute of Parasitology and Biomedicine "López-Neyra", Spanish National Research Council (CSIC), Granada E-18016, Spain
[c] ECsens, Department of Analytical Chemistry, Faculty of Sciences, University of Granada, E-18071 Granada, Spain
[d] Departamento de Química Inorgánica, Facultad de Ciencias, Universidad de Granada, E-18071 Granada, Spain
[e] Departamento de Química Inorgánica y Analítica, E.S.C.E.T., Universidad Rey Juan Carlos, E-28933 Móstoles, Madrid, Spain

ARTICLE INFO

Article history:
Received 5 December 2013
Accepted 25 February 2014
Available online xxxx

Keywords:
Cytotoxicity
Toxicity
Lanthanide
Cinnamate
Phenylacetate
Styrene oxidation

ABSTRACT

Eleven lanthanide compounds [Y(cinn)$_3$] (**1**), [La(cinn)$_3$] (**2**), [La(4-OMecinn)$_3$]·2H$_2$O (**3**), [La(4-Clcinn)$_3$]·2H$_2$O (**4**), [La(4-OMephac)$_3$]·4H$_2$O (**5**), [La(4-Clphac)$_3$]·3H$_2$O (**6**), [Ce(cinn)$_3$] (**7**), [Nd(cinn)$_3$] (**8**), [Sm(cinn)$_3$]·H$_2$O (**9**), [Yb(cinn)$_3$] (**10**) and [Sm(4-OMephac)$_3$]·H$_2$O (**11**) containing carboxylato ligands (cinn = cinnamate; 4-OMecinn = 4-methoxicinnamate; Clcinn = 4-chlorocinnamate; 4-OMephac = 4-methoxyphenylacetate; 4-Clphac = 4-chlorophenylacetate) have been synthesized and characterized by elemental analysis, IR, ^{1}H and ^{13}C NMR spectroscopy, thermal analysis and X-ray diffraction powder patterns. In addition, compound **11** was characterized by single crystal X-ray diffraction studies. The cytotoxic activity of these complexes has been tested against three different human tumour cell lines HL60 (human promyelocytic leukemia), K562 (human erythromyeloblastoid leukemia) and MCF7 (breast cancer), observing a very modest cytotoxic activity for all tested compounds. In addition, toxicity tests to macrophages and erythrocytes have also been carried out, observing that none of the compounds is toxic against these immunocompetent cells. Finally, all the synthesized compounds have been tested as catalysts for styrene oxidation observing conversions higher than 50% after 19 h of reaction as well as a relatively high selectivity to two main products benzaldehyde (BzA) and 1-phenylethane-1,2-diol (PhED). Complex **7** presents the higher conversion (99.56%) with a relatively high selectivity towards PhED of 72.07%.

1. Introduction

Metal coordination complexes have shown interesting physico-chemical properties which have been exploited not only in homogeneous catalysis or in the preparation of novel materials with fascinating properties, but also in medicinal purposes as cytotoxic agents [1]. Lanthanide complexes have also attracted attention in pharmaceutical applications due to the results presented in recent research [2–6]. Especially, studies on cinnamic acid derivatives have shown anti-tumoral properties [7–12], attracting the interest of the scientists because they could be employed as potential drugs.

In addition, lanthanide complexes possess unique properties that make them attractive and promising for research, in both stoichiometric and catalytic reactions. The particular combination of their ionic radii, the Lewis acidity and the presence of unemployed 5d and 6s orbitals, provide a great advantage in coordination complexes. A remarkable variation of the ionic radius of the lanthanide series, gives the possibility of adjusting the geometrical parameters of the metal coordination sphere, optimizing the selectivity for choosing the central atom of the substrate with a radius appropriate to the specifications of the catalytic reaction [13].

Thus, another common application of lanthanide complexes may be their use as catalyst for the preparation of different compounds and/or materials. Many studies of the oxidation and epoxidation of organic substrates with lanthanide complexes have been

* Corresponding authors. Tel.: +34 914888507; fax: +34 914888143 (S. Gómez-Ruiz).
E-mail addresses: santiago.gomez@urjc.es (S. Gómez-Ruiz), dorian.polo@correounivalle.edu.co (D. Polo-Cerón).

http://dx.doi.org/10.1016/j.poly.2014.02.040
0277-5387/

reported [14–17], and for basic chemistry, the study of the oxidation of styrene is interesting because it is the simplest vinyl aromatic derivative and the catalytic studies may be the basis for further research, for example to the cosmetics industry, flavorings and pharmaceuticals [18–22].

Thus, having in mind the potential application of lanthanide complexes in biologic and catalytic processes and based on previous reports by our group on the application of metal complexes with biological activity [23,24], and catalytic properties of metal complexes [25,26], we report here the synthesis and characterization of Y(III), La(III), Ce(III), Nd(III), Sm(III) and Yb(III) complexes with *p*-substituted-cinnamate and *p*-substituted phenylacetate ligands (Fig. 1) and the toxicity against immunocompetent cells (mice macrophages and erythrocytes) and cytotoxicity against specific human cancer cells line (HL60 (human promyelocytic leukemia), K562 (human erythromyeloblastoid leukemia) and MCF7 (breast cancer). In addition, the study of the catalytic activity and selectivity of these compounds on styrene oxidation is reported.

2. Experimental

2.1. Materials and methods

trans-Cinnamic acid (cinnH), 4-methoxycinnamic acid (4-OMecinnH), 4-chlorocinnamic acid (4-ClcinnH), 4-methoxyphenylacetic acid (4-OMephacH), 4-chlorophenylacetic acid (4-ClphacH) and $LnCl_3\ xH_2O$ (Ln = Y, La, Ce, Nd, Sm, Yb) were purchased from Sigma–Aldrich and other chemicals were obtained commercially and used without further purification. The sodium cinnamates were synthesized in an equimolar reaction by the neutralization of the respective acid with NaOH solution in ethanol, the mixture was held at room temperature for 1 h with constant stirring, the solid obtained was filtered, washed with ethanol:water (1:1) and dried under vacuum. For synthesis of sodium 4-methoxyphenylacetate and sodium 4-chlorophenylacetate, the methodology described above was performed using pentane and ethyl acetate as solvents respectively. Microanalyses were carried out with a Flash EA 1112 Series CHN Analyzer. Metal concentrations were determined by EDTA titration. Infrared spectra were recorded with a NICOLET 6700 Spectrometer (4000–225 cm^{-1} with recording accuracy of 1 cm^{-1}). ^1H NMR and ^{13}C NMR spectra were recorded in DMSO-d^6 at 25 °C on a Bruker Avance II 400 spectrometer. Chemical shifts are recorded in δ values (ppm) respect to residual signals of deuterated solvents and coupling constants (J) are given in Hz. The multiplicities of carbon signals were obtained from distortionless enhancement by polarization transfer experiments (DEPT). Powder X-ray diffractograms of different samples were recorded on Panalytical X'Pert PRO X-ray diffractometer equipped with a Co Kα radiation source. The scanning range used was at least $2\theta = 5–40°$ at at 0.02° s^{-1} with a 0.25° divergence slit, 0.04 rad soller slit, 0.76 mm anti-scatter slit and a Fe filter. All scans were run at room temperature and powder patterns were generated by using X'Pert Data Collector software. TG-DTG analyses were performed with the NETZSCH STA 409 simultaneous thermal analyzer. Heating was conducted under static condition in air with a range of 298–1073 K at 10 K min^{-1}.

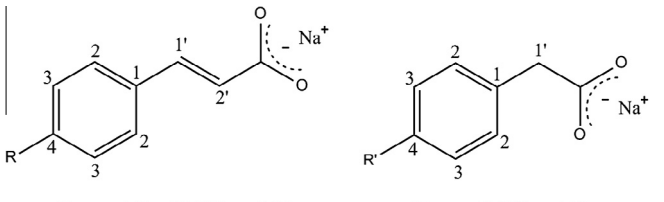

Fig. 1. The structural formula of the sodium ligand precursors (NaL): (a) sodium cinnamate Na(cinn), (b) sodium 4-methoxycinnamate Na(4-OMecinn), (c) sodium 4-chlorocinnamate Na(4-Clcinn), (d) sodium 4-methoxyphenylacetate Na(4-OMephac) and (e) sodium 4-cholorophenylacetate Na(4-Clphac).

2.2. Synthesis of lanthanide compounds

The Ln(III) complexes were prepared by using similar methods to those described in literature [27,28] (Fig. 2).

2.2.1. Synthesis of $[Y(cinn)_3]$ (**1**)

An aqueous solution (10 ml) of Na(cinn) (3 eq: 842 mg, 4.95 mmol) was slowly added to the aqueous solution (15 ml) of $YCl_3{\cdot}6H_2O$ (500 mg, 1.65 mmol) and a precipitate formed instantly. Upon the addition of the sodium salt, the solution was adjusted to pH 5 with drops of 0.1 M HCl or NaOH solution, controlled by pH-meter, then stirred for 3 h and filtered. The white precipitate was then washed with distilled water and dried in a desiccator for 2 days. Yield: 730 mg, 83 %. $C_{27}H_{21}YO_6$, Elemental analysis; C, 58.50 (calc. 61.15); H, 3.99 (3.99); Y, 16.54 (16.76)%. IR (KBr pellet cm^{-1}): 3033 w, 2924 w, 1638 s, 1597 m, 1516 s, 1451 m, sh, 1412 s, 1386 s, 1290 w, 1237 s, 1177 w, 1071 w, 987 s, 876 s, 852 w, 779 s, 749 m, 724 m, 686 s, 593 s, 554 m, 484 m. ^1H NMR (DMSO-d^6) δ (ppm) 6.51 (d, 3H, ^3J = 15.61 Hz, H-2′), 7.33 (s, 9H, H-3 and H-4 overlapped), 7.49 (d, 3H, ^3J = 16.00 Hz, H-1′), and 7.56 (d, 6H, ^3J = 2.34 Hz, H-2); ^{13}C NMR δ (ppm) 124.87 (C-2′), 128.13 (C-4), 129.24 (C-2), 129.77 (C-3), 135.64 (C-1), 136.42 (C-1′), and 176.86 (C=O). Powder XRD [d-spacings/Å (I/I°)]- 12.93 (100), 11.46 (72), 8.95 (39), 8.33 (35), 6.51 (58), 5.93 (17), 5.85 (19), 5.75 (21), 5.50 (17), 5.40 (11), 5.13 (10), 4.70 (15), 4.65 (33), 4.46 (42), 4.16 (15), 3.97 (33), 3.89 (21), 3.71 (21).

2.2.2. Synthesis of $[La(cinn)_3]$ (**2**)

The synthesis of **2** was carried out in identical manner to **1**. White powder, yield: 750 mg, 96%. $C_{27}H_{21}LaO_6$, Elemental analysis; C, 55.47 (calc. 55.88); H, 3.95 (3.65); La, 23.71 (23.93)%. IR (KBr pellet cm^{-1}): 3051 w, 1636 s, 1575 m, 1529 m, sh, 1499 s, 1450 m, 1394 s, 1289 w, 1243 s, 1200 w, 1071 w, 982 s, 879 m, 850 m, 779 s, 737 s, 688 m, 589 s, 539 m, 482 m. ^1H NMR (DMSO-d^6) δ (ppm) 6.47 (d, 3H, ^3J = 16.06 Hz, H-2′), 7.31 (s, 9H, H-3 and H-4 overlapped), 7.43 (d, 3H, ^3J = 15.81 Hz, H-1′), and 7.53 (d, 6H, ^3J = 2.76 Hz, H-2); ^{13}C NMR δ (ppm) 125.62 (C-2′), 127.51 (C-4), 128.72 (C-2), 129.07 (C-3), 135.31 (C-1), 139.89 (C-1′), and 176.62 (C=O). Powder XRD [d-spacings/Å (I/I°)]- 11.89 (100), 8.99 (6), 6.54 (29), 5.67 (28), 4.50 (9), 4.28 (22), 3.92 (10), 3.88 (4), 3.78 (5), 3.51 (5), 3.36 (4), 3.27 (6), 3.14 (8), 2.99 (8), 2.64 (4). TGA mass loss 44.00% (295–500 °C, 1 step, calc. La_2O_3 formation = 43.86 %).

2.2.3. Synthesis of $[La(4\text{-}OMecinn)_3]{\cdot}2H_2O$ (**3**)

The synthesis of **3** was carried out in identical manner to **1**. White powder, yield: 800 mg, 84%. $C_{30}H_{31}LaO_{11}$, Elemental analysis; C, 49.81 (calc. 51.00); H, 4.37 (4.42); La, 19.79 (19.66)%. IR (KBr pellet cm^{-1}): 3342 m, br, 2935 w, 2837 w, 1638 s, 1606 s, 1573 w, 1513 s, 1426 s, 1404 s, 1305 m, 1246 s, 1174 s, 1109 m, 1032 s, 985 s, 879 m, 832 s, 781 m, 722 m, 558 m, 519 w, 268 s, 238 s. ^1H NMR (DMSO-d^6) δ (ppm) 3.73 (s, 9H, –O–CH_3), 6.35 (d, 3H, ^3J = 15.65 Hz, H-2′), 6.83 (d, 6H, ^3J = 7.34 Hz, H-3), 7.41 (d, 3H, ^3J = 16.14 Hz, H-1′), and 7.45 (d, 6H, ^3J = 8.31 Hz, H-2); ^{13}C NMR δ (ppm) 55.65 (–O–CH_3), 114.64 (C-3), 123.40 (C-2′), 128.36 (C-1), 129.62 (C-2), 140.50 (C-1'), 160.55(C-4), and 177.30 (C=O). Powder XRD [d-spacings/Å (I/I°)]- 24.21 (100), 9.36 (14), 8.49 (4), 7.61 (19), 7.24 (17), 7.02 (64), 5.89 (7), 5.53 (9), 4.66 (13), 4.44 (4), 4.29 (4), 4.04 (5), 3.80 (5). TGA mass loss 4.89% (70–120 °C, 1

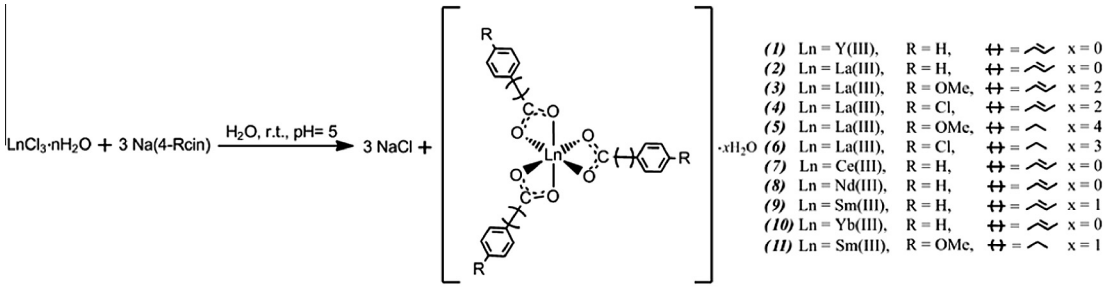

Fig. 2. Synthetic method for the preparation of La(III) complexes with cinnamate and phenylacetate ligands.

step, calc. 2 × H_2O = 5.10%), 41.90% (300–600 °C, 2 steps, calc. $La_2O_2CO_3$ formation = 44.84%).

*2.2.4. Synthesis of [La(4-Clcinn)$_3$]·2H_2O (**4**)*

The synthesis of **4** was carried out in identical manner to **1**. White powder, yield: 780 mg, 81%. $C_{27}H_{22}Cl_3LaO_8$, Elemental analysis; C, 44.81 (calc. 45.06); H, 2.93 (3.08); La, 19.80 (19.30)%. IR (KBr pellet cm^{-1}): 3410 w, br, 1639 s, 1572 m, 1509 vs 1494 sh, 1423 vs 1398 s, 1285 w, 1249 m, 1092 s, 1012 m, 983 s, 828 vs 749 m, 720 m, 664 w, 554 w, 541 w, 499 m, 455 m, 266 m, 243 m. ^{1}H NMR (DMSO-d^6) δ (ppm) 6.48 (d, 3H, ^3J = 16.14 Hz, H-2′), 7.35 (d, 6H, ^3J = 7.83 Hz, H-3), 7.41 (d, 3H, ^3J = 16.14 Hz, H-1′), and 7.55 (d, 6H, ^3J = 7.83 Hz, H-2); ^{13}C NMR δ (ppm) 125.75 (C-2′), 129.23 (C-3), 129.80 (C-2), 134.23 (C-1), 134.53 (C-4), 139.76 (C-1′), and 175.07 (C=O). Powder XRD [d-spacings/Å (I/I°)]- 22.09 (100), 10.74 (31), 7.30 (15), 6.63 (10), 6.14 (4), 5.47 (14), 5.43 (19), 5.37 (7), 4.84 (19), 4.10 (9), 3.97 (4), 3.63 (15), 3.25 (11), 2.72 (8). TGA mass loss 4.51% (80–125 °C, 1 step, calc. 2 × H_2O = 5.01 %), 15.00% (160–320 °C, 2 steps, calc. 3 × Cl [La(cinn)$_3$ formation] = 15.11%), 34.20% (330–550 °C, 1 step, calc. $La_2O_2CO_3$ formation = 36.28%).

*2.2.5. Synthesis of [La(4-OMephac)$_3$]·4H_2O (**5**)*

The synthesis of **5** was carried out in identical manner to **1**. White powder, yield: 740 mg, 78%. $C_{27}H_{35}LaO_{13}$, Elemental analysis; C, 45.30 (calc. 45.90); H, 4.75 (4.99); La, 19.97 (19.66)%. IR (KBr pellet cm^{-1}): 3221 m, br, 2959 w, 2836 w, 1557 s, 1516 s, 1431 s, 1401 s, 1283 m, 1248 s, 1179 m, 1108 w, 1034 m, 937 w, 822 m, 733 m, 697 m, 568 w, 259 m, 236 m. ^{1}H NMR (DMSO-d^6) δ (ppm) 3.26 (s, 6H, H-1′), 3.71 (s, 9H, –O–CH_3), 6.79 (d, 6H, ^3J = 8.53 Hz, H-3), and 7.14 (d, 6H, ^3J = 8.53 Hz, H-2); ^{13}C NMR δ (ppm) 43.55 (C-1′), 54.95 (–O–CH_3), 113.17 (C-3), 129.21 (C-1), 130.36 (C-2), 157.39 (C-4), 181.67 (C=O). Powder XRD [d-spacings/Å (I/I°)]- 9.77 (82), 8.73 (29), 7.97 (33), 6.52 (100), 6.11 (6), 5.22 (7), 4.89 (8), 4.71 (7), 4.59 (4), 4.36 (4), 4.26 (14), 3.99 (9), 3.20 (5), 3.05 (6), 2.79 (4), 2.76 (6), 2.42 (7), 2.16 (5). TGA mass loss 10.41% (50–125 °C, 1 step, calc. 4 × H_2O = 10.20%), 50.06% (300–530 °C, 1 step, calc. La_2O_3 formation = 48.63%).

*2.2.6. Synthesis of [La(4-Clphac)$_3$]·3H_2O (**6**)*

The synthesis of **6** was carried out in identical manner to **1**. White powder, yield: 780 mg, 83%. $C_{24}H_{24}LaCl_3O_9$, Elemental analysis; C, 39.19 (calc. 41.08); H, 3.32 (3.45); La, 19.48 (19.80)%. IR (KBr pellet cm^{-1}): 3410 m, br, 2915 w, 1544 vs 1493 m, 1422 s, 1397 vs 1288 s, 1202 w, 1177 w, 1092 s, 1017 m, 934 w, 857 m, 810 s, 743 s, 685 s, 633 w, 581 m, 504 m, 469 m, 302 w, 277 w, 259 m, 231 w. ^{1}H NMR (DMSO-d^6) δ (ppm) 3.32 (s, 6H, H-1′), 7.21 (d, 6H, ^3J = 8.78 Hz, H-3), and 7.24 (d, 6H, ^3J = 8.53 Hz, H-2); ^{13}C NMR δ (ppm) 43.58 (C-1′), 127.58 (C-3), 130.34 (C-1), 131.27 (C-2), 136.15 (C-4), 180.80 (C=O). Powder XRD [d-spacings/Å (I/I°)]- 9.40 (26), 8.96 (100), 8.32 (45), 8.09 (5), 6.48 (33), 5.97 (49), 5.04 (8), 4.94 (5), 4.70 (5), 4.61 (6), 4.48 (5), 4.05 (6), 3.68 (6), 3.48 (7), 2.85 (7). TGA mass loss 8.12% (55–120 °C, 1 step, calc. 3 × H_2O = 7.70%), 49.30% (300–450 °C, 1 step, calc. La_2O_3 formation = 49.70%).

*2.2.7. Synthesis of [Ce(cinn)$_3$] (**7**)*

The synthesis of **7** was carried out in identical manner to **1**. Pale yellow powder, yield: 710 mg, 91%. $C_{27}H_{21}CeO_6$, Elemental analysis; C, 54.54 (calc. 55.76); H, 4.03 (3.64); Ce, 24.37 (24.09)%. IR (KBr pellet cm^{-1}): 3050 w, 1636 s, 1575 w, 1529 m, 1499 vs 1450 m, 1395 vs 1290 w, 1243 s, 982 s, 879 m, 850 m, 779 s, 737 s, 688 m, 589 s, 540 m, 481 w. Powder XRD [d-spacings/Å (I/I°)]- 11.31 (100), 6.53 (39), 5.66 (30), 5.41 (2), 4.48 (12), 4.28 (27), 3.91 (6), 3.77 (5), 3.67 (3), 3.49 (3).

*2.2.8. Synthesis of [Nd(cinn)$_3$] (**8**)*

The synthesis of **8** was carried out in identical manner to **1**. Pale blue powder, yield: 690 mg, 85%. $C_{27}H_{21}NdO_6$, Elemental analysis; C, 53.21 (calc. 55.37); H, 3.83 (3.61); Nd, 24.86 (24.63)%. IR (KBr pellet cm^{-1}): 3053 w, 1636 s, 1575 m, 1530 m, 1500 vs 1450 m, 1398 vs 1290 w, 1244 s, 1201 w, 1072 w, 983 s, 879 m, 850 m, 780 s, 742 s, 688 m, 589 s, 540 m, 483 m. Powder XRD [d-spacings/Å (I/I°)]- 11.21 (100), 6.53 (29), 5.66 (29), 5.38 (7), 4.47 (25), 4.28 (20), 3.90 (11), 3.77 (4), 3.63 (4), 3.46 (3), 3.35 (4), 3.27 (5).

*2.2.9. Synthesis of [Sm(cinn)$_3$]·H_2O (**9**)*

The synthesis of **9** was carried out in identical manner to **1**. Beige powder, yield: 740 mg, 88%. $C_{27}H_{23}SmO_7$, Elemental analysis; C, 53.27 (calc. 53.18); H, 3.49 (3.80); Sm, 24.88 (24.66)%. IR (KBr pellet cm^{-1}): 3422 w, br,3054 w, 1636 s, 1576 m, 1500 vs 1449 m, 1394 vs 1291 w, 1243 s, 1200 w, 1073 w, 983 s, 880 m, 850 m, 780 s, 743 s, 730 m, sh, 689 m, 589 s, 542 m, 482 m, 371 m, 335 m, 282 m, 251 m, 236 m, 227 s. Powder XRD [d-spacings/Å (I/I°)]- 11.47 (100), 6.53 (31), 5.65 (29), 5.36 (7), 4.45 (9), 4.28 (23), 3.89 (11), 3.77 (10), 3.61 (7), 3.44 (4), 3.34 (5), 3.27 (5), 3.14 (7).

*2.2.10. Synthesis of [Yb(cinn)$_3$] (**10**)*

The synthesis of **10** was carried out in identical manner to **1**. White powder, yield: 630 mg, 79%. $C_{27}H_{21}YbO_6$, Elemental analysis; C, 50.25 (calc. 52.77); H, 3.35 (3.44); Yb, 28.84 (28.16)%. IR (KBr pellet cm^{-1}): 3028 w, 1636 vs 1577 s, 1518 vs 1452 vs sh,1419 vs 1291 m, 1253 s, 1238 s, 1204 w, 1180 w, 1072 w, 985 s, 876 s, 852 w, 779 s, 747 s, 725 m, 686 s, 592 s, 556 m, 485 m. Powder XRD [d-spacings/Å (I/I°)]- 12.96 (100), 11.50 (31), 8.95 (22), 8.31 (25), 6.49 (57), 5.84 (8), 5.76 (6), 5.48 (14), 5.42 (4), 5.12 (6), 4.69 (4), 4.46 (8), 4.16 (6), 3.96 (19), 3.89 (5), 3.75 (4), 3.67 (6), 3.19 (5), 3.07 (6).

*2.2.11. Synthesis of [Sm(4-OMephac)$_3$]·H_2O (**11**)*

The synthesis of **11** was carried out in identical manner to **1**. White powder, yield: 690 mg, 76%. $C_{29}H_{29}SmO_{10}$, Elemental analysis; C, 48.71 (calc. 48.85); H, 4.24 (4.40); Sm, 22.55 (22.65)%. IR

(KBr pellet cm^{-1}): 3435 m,br, 2959 w, 2835 w, 1616 m, 1537 s, 1516 s, 1432 m, 1402 m, 1285 w, 1249 m,sh, 1177 m, 1106 w, 1035 m, 820 w, 794 w, 732 w, 700 w, 616 w, 476 w. Powder XRD [d-spacings/Å (I/I°)]- 9.57 (82), 7.93 (29), 7.22 (33), 6.99 (100), 6.22 (6), 5.67 (7), 5.03 (8), 4.79 (7), 4.66 (4), 4.11 (4), 3.78 (7), 3.51 (5).

2.3. Cytotoxic activity

2.3.1. Tumor cell culture

HL60 (human promyelocytic leukemia) and K562 (human erythromyeloblastoid leukemia) cell lines in suspension and MCF7 (breast cancer) as monolayer were maintained in RPMI-1640 culture medium (Gibco) supplemented with 10% heat inactivated fetal bovine serum (FBS, Gibco), 1% penicillin/streptomycin (Invitrogen) and 1% L-glutamine (Invitrogen) at 37 °C in a humidified atmosphere of 5% (v/v) CO_2.

2.3.2. Cytotoxicity assay

The cytotoxic activity of the compounds was evaluated using the Alamar Blue assay that has been previously demonstrated to be a rapid and inexpensive method for the medium through put screening of compounds [29]. The Alamar Blue oxidation–reduction dye is a common used indicator of cell viability. The blue, non-fluorescent compound, Resazurin, is reduced to the pink, fluorescent Resorufin within the cytoplasm of a viable cell, and the fluorescence is directly proportional to cell number. In short, HL60, K562 and MCF7 exponentially growing cells were seeded into 96-well plates on day 0 at 10 000 cells/well to prevent cell confluence during the period of experiment.

All stock compounds (**1**–**9**) solutions (30 mM) were prepared in 100% DMSO (Sigma) and stock solution of **10** was prepared in Ethanol (100%). A first dose of increasing concentrations of the studied compounds (**1**–**10**) was added to each well per triplicate at 37 °C. After 24 h, cells were treated with a second dose of the compounds and kept for 96 h at 37 °C. Final concentrations achieved in treated wells were 10, 20, 30, 50, 100, 200, 350, 550, 750 and 1000 μM for each suspension. Equal concentrations of vehicle were added and served as control wells. The percentage of surviving cells relative to untreated controls was calculated 96 h after the beginning of compounds exposure. After 96 h treatment, we added ready-to-use solution of Resazurin (100X in PBS) to each well and kept the plates were kept in darkness conditions at 37 °C. After 4 h incubation 100 μL of 3% sodium dodecyl sulfate (SDS) was added to each well of the plate to end the Resazurin reaction. Fluorescence was measured with a excitation λ of 550 nm and emission at 590 nm using a 96-well plate reader (Infinite F200 Tecan Fluorimeter). The IC_{50} value was defined as the percentage of the compound at which 50% cell toxicity was observed. Data from this study were analyzed with GraphPad Prism 5.0 and OriginLab Pro 8 software.

2.3.3. Isolation of murine peritoneal macrophages

Healthy 6 weeks old C57BL/6 mice were used for extraction of macrophages from the peritoneal cavity. C57BL/6 mice were euthanized under CO_2 gas and around 5 mL of cold harvest RPMI 1640 medium was injected into the peritoneal region of the mice. A massage in the peritoneal region of the mouse was performed during the next 5 min to allow the cells to detach from the peritoneal wall. Rapidly, the peritoneal fluid was removed and dispensed into a 50 mL conical polypropylene centrifuge tube on ice. The peritoneal exudate cells were centrifuged in a refrigerated centrifuge 10 min at 2000 rpm at 4 °C. A density of 100 000 macrophages per well was plated into a 96-well plate and kept at 37 °C in a humidified atmosphere of 5% (v/v) CO_2. After 2 h in culture the complete cultured medium (RPMI 1640,1 % Penicillin/Streptomycin, 10% FBS) was changed and the plate was kept at 37 °C. After one day of culture, peritoneal macrophages were treated with increasing concentrations of the studied compounds (50, 300, 750 and 950 μM) and the corresponding vehicle solutions (DMSO and EtOH). After 96 h of treatment Alamar Blue cytotoxicity test was performed as described above (see cytotoxicity assay section). Compounds toxicity to macrophages was considered acceptable if the fluorescence was within 80% of that observed for the untreated macrophages.

2.3.4. Hemolysis assay

Approximately 400 μL of blood was carefully extracted with a syringe-connected needle from C57BL/6 mice previously euthanized by cardiac puncture and added to a 1.5 mL eppendorf containing 4% Sodium Citrate (120 μL). Several blood dilutions were prepared in PBS (3 × 1:20). The blood suspension was then diluted with 2% (v/v) citrate in PBS and erythrocytes were counted with a Neubauer camera. A density of 10 x 10^6 erythrocytes (125 μL) was added to centrifuge tubes and then treated with different concentrations of compounds (**1**–**10**) (250, 550, 750 and 950 μM) and vehicle solutions (DMSO and EtOH). Hemolysis 0% (Blank) was prepared by mixing both blood and PBS solutions (1:1) and hemolysis 100% was achieved by mixing blood solution and 0.1 % Triton. The tubes were incubated for 1 h at 37 °C under continuous agitation. After incubation period, erythrocytes were separated by centrifugation (1000*g*, at room temperature, 5 min). A 100 μL portion of each supernatant was further transferred to a 96-well plate to measure the absorbance at 540 nm into a microplate reader (Versamax tunable, Molecular devices). All values were normalized to the control untreated (PBS) samples.

2.4. Catalytic oxidation of styrene

Catalytic reactions were carried out in a condensation system with stirrer, using acetonitrile as solvent and hydrogen peroxide solution as oxidant. A mixture of styrene (10.0 mmol), lanthanide catalyst (0.01 mmol) and solvent (10.0 mL) was stirred for few minutes at room temperature. H_2O_2 (17.6 mmol) was then added and the reaction mixture was stirred for 19 h at 70 °C. Analysis of the content of the reaction mixtures were carried out in duplicate with an Agilent 6890 series GC (Gas Chromatography system) with a flame ionization detector (FID). Injection conditions were: injector temperature at 280 °C, FID detector at 295 °C with a ramp starting at 70 °C, then the temperature increases by 15 °C/min until reaching 220 °C (2 min) and finally, a rate of 10 °C/min until reaching 270 °C (3 min). Helium was used as carrier gas with a pressure of 9.5 Psi, a flow of 1.8 mL/min and a HP-INNOWax 19091 N-133 column (30 m × 0,25 mm, 0,25 μm). Oxidation products of styrene were identified (mass spectra) using a gas chromatography system coupled to a mass spectrometer SHIMADZU GCMS-QP2010, technique electron impact ionization (EI) at 70 eV.

2.5. Single-crystal structure determination

It should be noted that all crystals undergo a very fast degradation when they are removed from the mother liquor which has a high impact on the quality of the data. Several crystals of **11** were measured and the structure was solved from the best data we were able to collect. A suitable crystal of **11** was mounted on a glass fibre and used for data collection on a Bruker AXS APEX CCD area detector equipped with graphite monochromated Mo Kα radiation (λ = 0.71073 Å) by applying the ω-scan method. Lorentz-polarization and empirical absorption corrections were applied [30]. The structure was solved by direct methods and refined with full-matrix least-squares calculations on F^2 using the program SHELXS-97 [31]. Anisotropic temperature factors were assigned to all atoms. Hydrogen atoms bonded to water molecules could not be reliably

positioned, but the rest of the hydrogen atoms were treated as riding atoms using the SHELX-97 default parameters. Refinement reduced R_1 to 0.0506. Final $R(F)$, $wR(F^2)$ and goodness of fit agreement factors, details on the data collection and analysis can be found in Table S1 (Electronic Supplementary material). Selected bond lengths are given in Table S2 (ESI).

3. Results and discussion

3.1. Synthesis and characterization of lanthanide complexes

The Ln(III) complexes **1**–**11** were isolated as crystalline solids, soluble in DMSO, and mildly soluble in DMF and acetone, but only sparingly soluble in water and ethyl acetate. The results obtained by elemental analysis (carbon and hydrogen), EDTA complexometry, and TG-DTG analysis, agree with all structures proposed. The X-ray powder patterns (Fig. 3) verified that the compounds have a crystalline structure, with evidence of the formation of an isomorphous series for [Ln(cinn)$_3$] (Ln = La, Ce, Nd and Sm). The highly similarity of d-spacings and relative intensities for both yttrium and ytterbium complexes indicate that they have similar carboxylate binding modes (see Experimental). The X-ray powder patterns are almost identical, and furthermore, match the patterns of the published single crystal structures of [Y(cinn)$_3$] and [Nd(cinn)$_3$] [28]. However, attempts to acquire single crystals suitable for X-ray crystallography were unsuccessful for complexes with cinnamate ligands.

On the other hand, we were able to obtain suitable crystals of compound **11** (with the 4-methoxyphenylacetate (4-OMephac), which were analyzed by single crystal X-ray diffraction studies. **11** crystallizes in the triclinic system and $P\bar{1}$ space group. The structure is formed by zig-zag chains (Fig. 4) built from Sm^{3+} metal centers coordinated through 4-metoxyphenylacetic acid (4-OMephac) ligands and crystallization water molecules. Two coordination modes of the ligand are evident in this complex, bidentate and tridentate bridging, forming an extended one-dimensional polymer along *b* axis.

The asymmetric unit contains four Sm^{3+} centers, twelve monoanionic ligands and four water molecules. Three tridentate bridging ligands link Sm1 with Sm2 and Sm3 with Sm4 with bond lengths of 3.867 and 3.851 Å, respectively. These distances are slightly shorter than the distances of 4.074 and 4.104 Å corresponding to Sm2–Sm3 and Sm1–Sm4 bridges, in which, these metallic atoms are bridged by two tridentate bridging ligands and one bidentate carboxylato ligand. The Sm^{3+} atoms have SmO_9 environments in which Sm2 and Sm4 centers are coordinated with oxygen atoms pertaining to six different (4-OMephac) ligands and one water molecule while Sm1 and Sm3 are coordinated only to six different (4-OMephac) ligands. Sm–O bond distances have values in the range of 2.364(4)–2.702(5) Å. Benzene rings in the structure are parallel with perpendicular dispositions among them with dihedral angles near to 4.65° and 75.57°, respectively. Chains running along the *b* axis are not isolated but connected by hydrogen bonds involving some carboxylate groups and crystallization water molecules. As a consequence of these hydrogen bond interactions (range of 2.755–2.940 Å) in the *ab* plane, metallic centers pertaining to different chains have an inter-chain distance value of 10.032 Å.

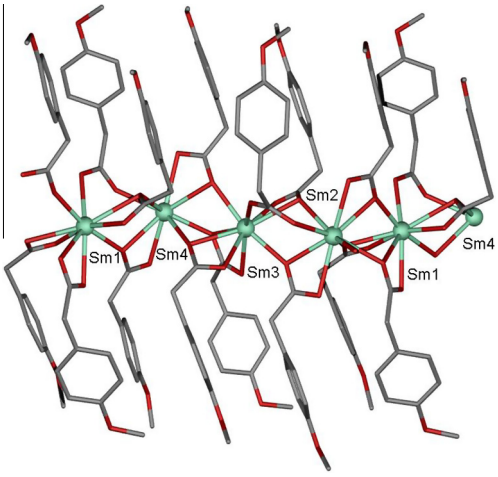

Fig. 4. X-ray molecular structure of compound **11**.

In the characterization of the compounds **1**–**11** by IR spectroscopy, several characteristic absorption bands of the cinnamate and phenylacetate ligands could be observed in the infrared spectra of the complexes, verifying coordination by the absence of

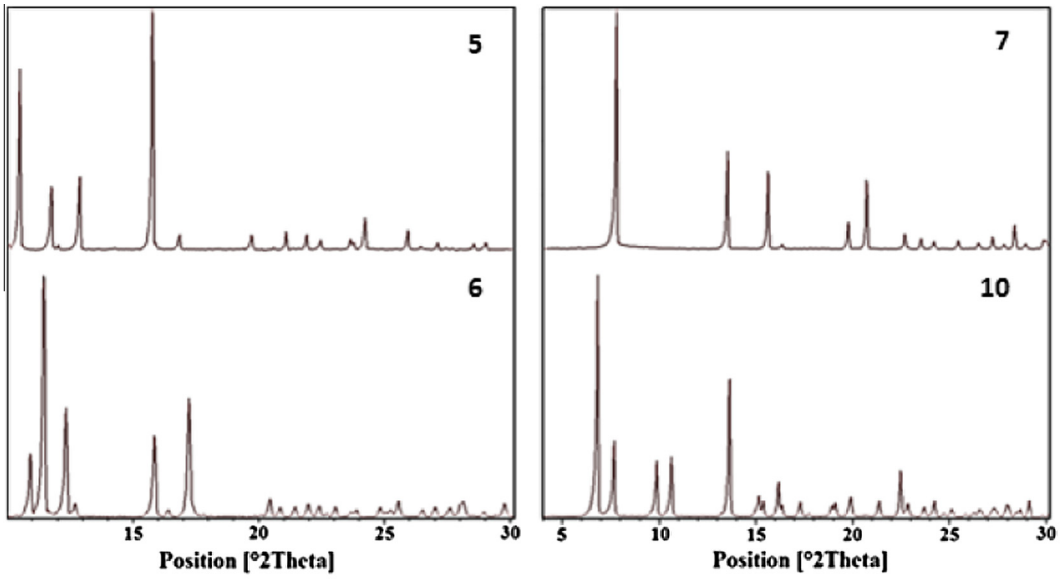

Fig. 3. X-ray powder diffraction patterns of the compounds: [La(4-OMephac)$_3$]·4H$_2$O (**5**); [La(4-Clphac)$_3$]·4H$_2$O (**6**); [Ce(cinn)$_3$] (**7**) and [Yb(cinn)$_3$] (**10**).

ν(COOH) absorption bands from the corresponding acids. Table 1 presents experimental data obtained by IR spectroscopy. For the compounds **3**–**6**, **9** and **11** the bands in the 3600–3050 cm^{-1} region are assigned to the stretching of the OH group, $\nu(OH)_w$, from hydration water. For **1**–**4** and **7**–**10**, the bands in the 1642–1636 cm^{-1} region are assigned to the ν(C=C) vibrations, and are not affected compared to sodium salts, confirming that the metal ions are not coordinated with the π-electron system of the olefinic double bond [27,32].

Stretching of the Ln–O bond (metal-carboxylate) has been attributed to the ν(Ln–O) bands that have been reported for lanthanum complex [33], finding the frequency of this band is observed approximately at 779 cm^{-1}, shifted in complexes **3**–**6** and **11** due to the presence of substituents in the aromatic ring and the $(C{=}C)_{propenyl}$ bond. For all complexes, a bathochromic effect was observed in the stretching ν(COO) compared to the sodium salts. A significant decrease in the $\delta\nu_{COO}^{-}$ value confirms that the lanthanide ions are coordinated to the ligands through the oxygen atoms of the carboxylate groups, and the ligands acts as a bidentate chelating agent. Additionally, the difference between the asymmetric and symmetric vibrations of less than 200 cm^{-1} indicates bidentate coordination of the carboxylate ligand [34].

In the characterization of the complexes **1**–**6** by ^{1}H and ^{13}C NMR, the corresponding signals were observed. For **1**–**4** two doublets assigned to the olefinic protons at $\delta \approx 6.40$ and 7.40 ppm were observed while for **3**–**6** the signals attributed to the aromatic protons were found as two doublets observed in the aromatic region with ^{3}J between 7.3 and 8.8 Hz. A singlet at high field ($\delta \approx 3.70$ ppm) in ^{1}H NMR spectra of **3** and **5** was assigned to the methoxy group protons. Another characteristic signal for **5** and **6** is a singlet at $\delta \approx 3.30$ ppm, corresponding to the protons of the aliphatic chain of the ligand, verifying that these protons are not

Table 1
Selected IR bands of the sodium ligands and their Ln(III) complexes.

Compound	Main bands (cm^{-1})								
	$\nu(OH)_w$	ν(C=C)	ν_{as}(COO)	ν_s(COO)	$\delta\nu^{*}$	$\delta(C{-}H)_{ip}$	δ(=CH)	$\delta(C{-}H)_{op}$	ν(Ln–O)
NaL_1	–	1641	1548	1411	137	1244	970	773, 713	–
1	–	1638	1516	1412	104	1237	987	724, 686	779
2	–	1636	1500	1394	106	1243	982	736, 687	779
7	–	1636	1499	1395	104	1243	982	737, 688	779
8	–	1636	1500	1398	102	1244	983	742, 688	780
9	3422	1636	1500	1394	106	1243	983	743, 689	780
10	–	1636	1518	1419	99	1238	985	747, 686	779
NaL_2	–	1642	1547	1399	148	1241	971	829	–
3	3342	1638	1513	1404	109	1244	985	832	781
NaL_3	3424	1639	1562	1429	133	1238	970	827	–
4	3410	1639	1509	1398	111	1249	983	828	749
NaL_4	3411	–	1560	1404	156	1248	–	816	–
5	3221	–	1516	1401	115	1248	–	822	733
11	3435	–	1537	1402	135	1249	–	820	732
NaL_5	3441	–	1567	1390	177	1289	–	816	–
6	3410	–	1544	1422	122	1288	–	810	743

L_1 = (cinn), L_2 = (4-MeOcinn), L_3 = (4-Clcinn), L_4 = (4-OMephac), L_5 = (4-Clphac).
* $\Delta\nu_{COO}^{-} = \nu_{as}(COO^{-}) - \nu_s(COO^{-})$.

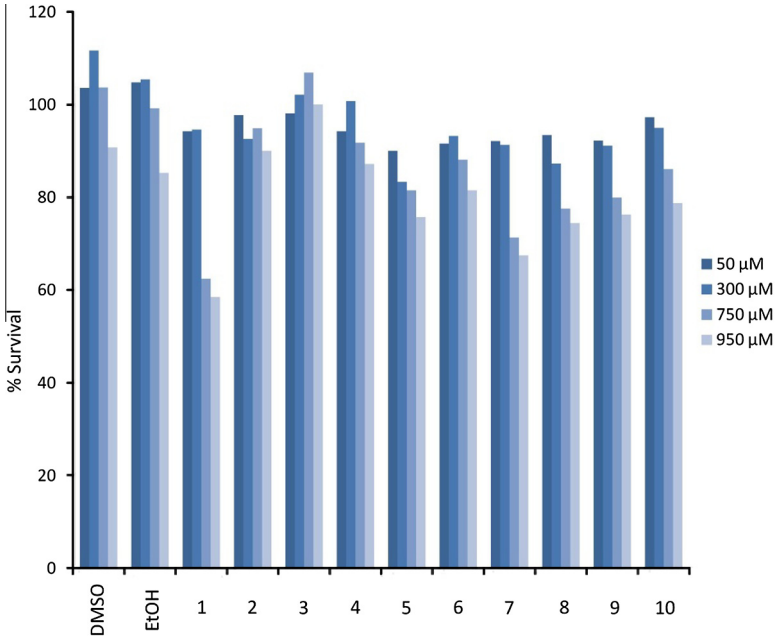

Fig. 5. Macrophage viability.

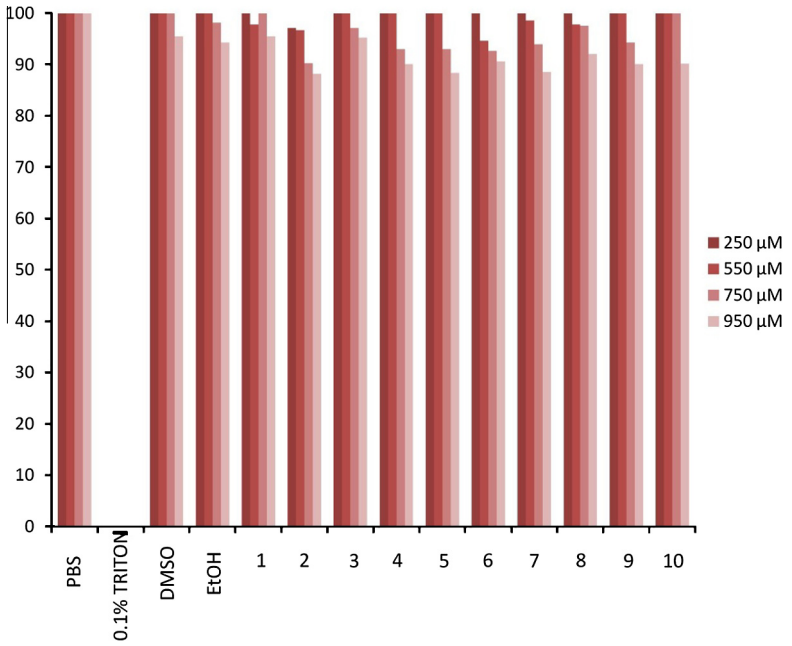

Fig. 6. Hemolysis assay. Erythrocytes viability.

Table 2
IC_{50} values (μM) after 96 h incubation with lanthanide compounds **1**–**10**.

Compound	IC_{50} values (μM)		
	HL60	K562	MCF7
1	>750	728.7 ± 1.1	>750
2	681.3 ± 5.0	>750	>750
3	577.9 ± 5.3	721.9 ± 1.2	>750
4	542.7 ± 5.0	629.2 ± 1.1	597.9 ± 2.0
5	>750	>750	>750
6	647.7 ± 4.0	>750	>750
7	672.5 ± 5.0	>750	>750
8	>750	>750	>750
9	>750	749.2 ± 1.1	>750
10	>750	>750	743.5 ± 1.1

being part of a conjugated system. Different types of carbons in the organic ligands were assigned in the ^{13}C NMR spectra. For all complexes, the carbonyl signal was observed at $\delta \approx 180$ ppm, while the carbon of the methoxy group for **3** and **5** were identified at 55 ppm. Quaternary carbons like C-1 and C-4 were verified when the corresponding signal disappeared by dept-135. For **5** and **6**, the secondary carbon of the aliphatic chain (C-1′), was observed in the dept-135 spectrum as a negative signal.

The thermal behavior of **2**–**6** was determined by TG-DTG analysis. Waters of hydration were calculated through mass loss in a step shown in the endothermic decomposition between 50 and 130 °C. Two stages of decomposition were identified: the decomposition of the anhydrous cinnamate to the dioxycarbonate, $La_2O_2CO_3$ [35,36], is observed between 300–600 °C for **3** and **4** complexes, and the sesquioxide (La_2O_3) formation was found for **2**, **5** and **6** complexes.

3.2. Biological studies

3.2.1. Toxicity to macrophages and erythrocytes

The *in vitro* toxicity of all the studied compounds (**1**–**10**) was firstly tested in primary cell culture of mice peritoneal macrophages and mice erythrocytes in order to determine whether lanthanide compounds could be used in preclinical trials against cancer cell lines.

The results showed that increasing doses (50, 300, 750 and 950 μM) of all the studied compounds (**1**–**10**) were practically non-toxic to macrophages as it can be clearly observed in Fig. 5. For the highest concentration (950 μM) of the studied compounds cell survivals higher than 60% were observed in all cases indicating an absence of toxicity to these cells.

Similarly, the hemolysis assay for the study of the erythrocyte viability using doses of the lanthanide compounds (**1**–**10**) of 250, 550, 750 and 950 μM showed cell survivals higher than 80% in all cases indicating that these compounds are non-toxic to red blood cells (Fig. 6).

3.2.2. Cytotoxicity studies against human cancer cell lines

In view of the very low, almost inexistent, toxicity of these compounds to macrophages and erythrocytes and with the aim to determine the potential use of these compounds as anticancer drugs, we decided to explore the *in vitro* cytotoxicity of **1**–**10** against HL60 (human promyelocytic leukemia), K562 (human erythromyeloblastoid leukemia) and MCF7 (breast cancer) cell lines by Alamar blue-based assays [29]. The IC_{50} values of the investigated compounds are summarized in Table 2.

The cytotoxicity experiments in cancer cells showed a dose-dependent toxic activity (Fig. 7) of the lanthanide compounds which began to be significant from 400 μM concentration. However, we observed that the cytotoxic activity of all the synthesized compounds was very low, showing IC_{50} values between 542.7 ± 5.0 and >750 μM, which corresponded to a non-toxic effect in human cancer cell lines. This result indicated that the studied lanthanide compounds are not appropriate for anticancer therapy, in contrast to some other lanthanide compounds [37].

3.3. Preliminary catalytic studies

3.3.1. Determination of the conversion rate and selectivity in the oxidation of styrene

In view of the low applicability of the synthesized lanthanide compounds as anticancer drugs, some catalytic applications were studied. Thus, the catalytic potential of the complexes **1**–**11** have been tested for the oxidation of styrene to give styrene oxide,

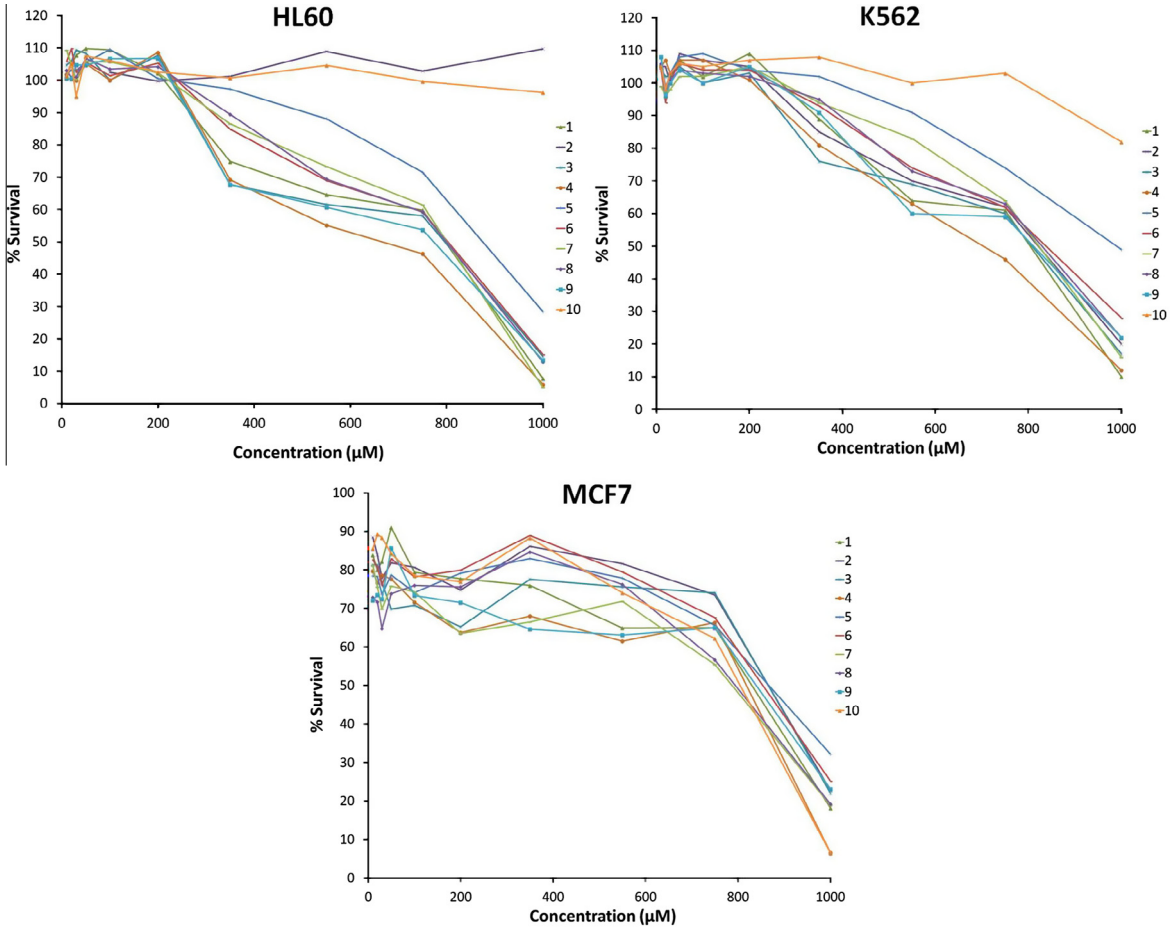

Fig. 7. Dose dependent cytotoxicity.

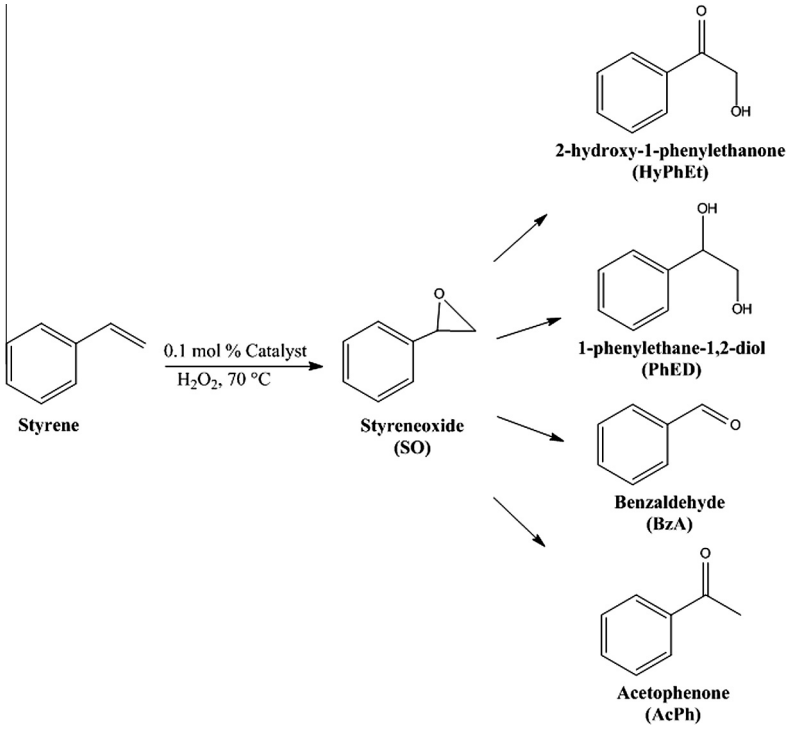

Fig. 8. Oxidation products of styrene with H_2O_2 catalyzed by lanthanide complexes with cinnamate and phenylacetate ligands.

Table 3
Effect of catalysts on the oxidation of styrene and the product selectivity.

Catalyst[a]	Conversion (%)	Selectivity (%)				
		BzA	SO	AcPh	HyPhEt	PhED
1	57.15	50.51	3.56	1.77	1.93	44.16
2	77.78	63.47	3.21	1.84	2.88	31.49
3	66.81	58.47	3.51	1.71	1.67	36.32
4	67.56	36.84	5.43	3.38	1.21	54.35
5	74.41	26.56	2.26	2.65	3.80	68.54
6	54.11	58.68	3.06	1.96	1.14	36.30
7	99.56	27.39	0.00	0.54	5.33	72.07
8	65.36	39.78	4.32	3.38	0.90	52.52
9	88.53	55.43	2.51	2.08	2.02	39.98
10	76.53	31.33	4.72	2.43	2.91	61.51
11	71.38	47.04	8.46	2.83	24.43	17.23

[a] Reaction conditions: styrene (1.04 g); catalyst (0.01 mmol); H_2O_2 (17.6 mmol); acetonitrile (10 mL), temperature 70 °C. Oxidation products were identified and quantified by Agilent 6890 series gas chromatographer equipped with an FID detector and a HP-INNOWax column.

benzaldehyde, 2-hydroxy-1-phenylethanone, 1-phenylethane-1,2-diol and acetophenone in presence of aqueous 30% H_2O_2 as oxidant (Fig. 8). The catalytic performances of all complexes are compared in Table 3, Figs. 9 and 10.

The effect of temperature variation, reaction time, catalyst:substrate ratio and oxidant:substrate ratio on the styrene conversion and product selectivity over all catalysts have been examined. All complexes proved to be catalytically active with conversions that exceeded 40% after 15 h of reaction. The relatively high selectivity to two main products (BzA and PhED) suggest that the complexes may be used as heterogeneous catalysts in other oxidation reactions, although a complete optimization of the reaction conditions would be necessary to obtain the best catalytic results.

As all experiments were conducted using similar conditions, in this preliminary study is possible to compare the effect of the metal in the oxidation reactions of styrene studied here. Clearly, Ce(III) complex (**7**) showed the highest activity reaching nearly 100% conversion with a relatively high selectivity (72%) towards 1-phenylethane-1,2-diol (PhED) (Table 3). This high activity may be due to redox reactions in where Ce(III) is easily oxidized to Ce(IV) by the oxidant of the reaction generating an intermediate which may increase the catalytic activity. Experimentally, Ce(III) complex was not recovered after the reaction, unlike the other compounds, in this case a yellow polymer product was observed after finishing reaction which was not characterized.

In the case of complexes **2**–**5**, **8** and **10**–**11**, they all have moderate activity (with conversion rates between 60 and 80%) using acetonitrile at 1:1000 (catalyst:styrene), 2:1 (peroxide:styrene), 15 h and 70 °C. It is also noteworthy that Sm(III) complex (**9**) showed high catalytic activity (89% conversion) and was used to study the influence of reaction time (see next Section 3.3.3). In addition, the study of the influence of the concentration of catalyst was conducted using the Ce(III) complex (**7**), while the oxidizing effect was studied for Nd(III) complex (**8**) (see Section 3.3.4).

3.3.2. Study of the influence of temperature

The response of the reaction towards an increase of the temperature has been studied and the results are presented in Fig. 9(a–c). It is clearly seen that the higher the temperature, the conversion increases at shorter times. At 85 °C all the catalysts with cinnamate ligands (without substituent) exceed 70% conversion after 8 h, however after 15 h, all exceed 80% conversion. At 55 °C the effect of the substituent in the La(III) complexes is observed. Complexes **4** and **6**, with 4-Clcinn and 4-Clphac ligands respectively, have higher conversion (>85%) after 15 h compared to the La(III) complexes with methoxy substituent on the aromatic ring or without substituent. In the selectivity to oxidation products, is generally found that at 55 °C the selectivity towards any specific products is less than at 85 °C. For complexes **3**–**7**, the major product is benzaldehyde (>75% selectivity) when the reaction takes place at 85 °C, whereas for complexes **1**, **2**, **8** and **10**, the major product is 2-hydroxy-1-phenylethanone. At studied temperatures a clear

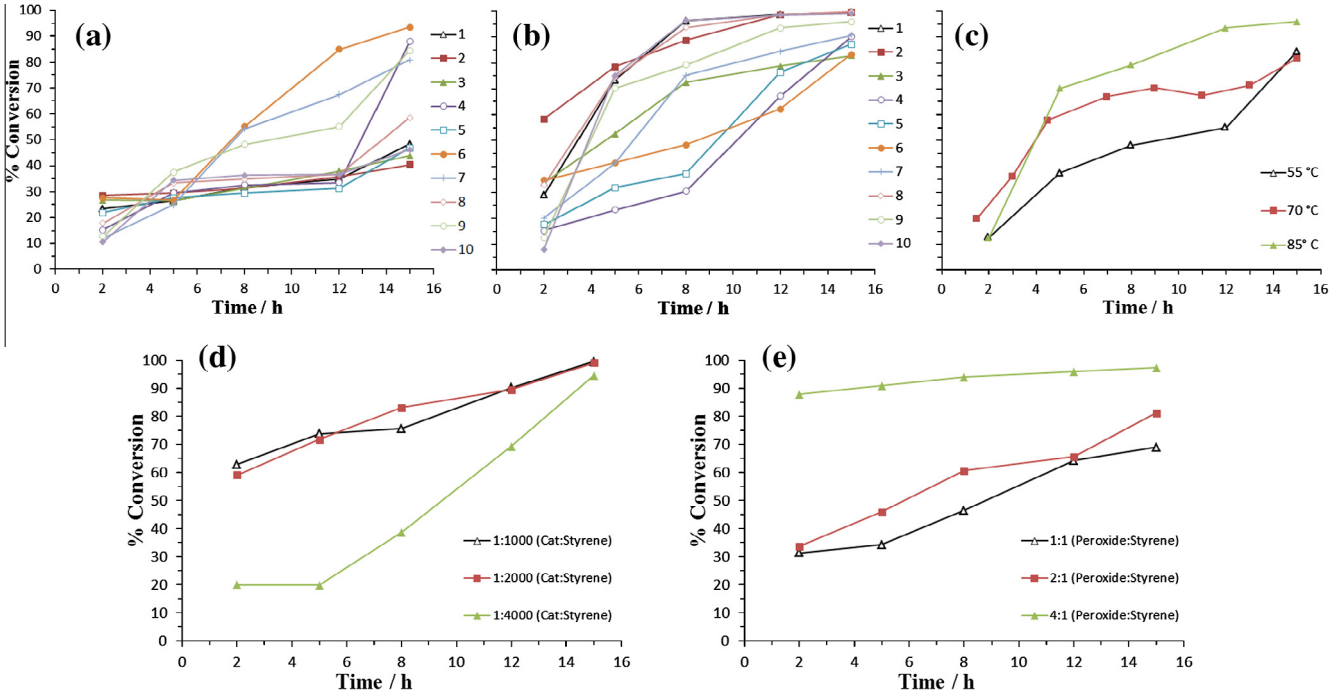

Fig. 9. Conversion rates in the oxidation of styrene at different times by using: (a) catalysts **1**–**10**, 1:1000 (catalyst:styrene), 2:1 (peroxide: styrene), 55 °C; (b) catalysts **1**–**10**, 1:1000 (catalyst:styrene), 2:1 (peroxide:styrene), 85 °C; (c) catalyst **9**, 1:1000 (catalyst:styrene), 2:1 (peroxide:styrene), 55, 70 and 85 °C; (d) catalyst **7**, 1:1000, 1:2000 and 1:4000 (catalyst:styrene), 2:1 (peroxide:styrene), 70 °C; (e) catalyst **8**, 1:1000 (catalyst:styrene), 1:1, 2:1 and 4:1 (peroxide:styrene), 70 °C.

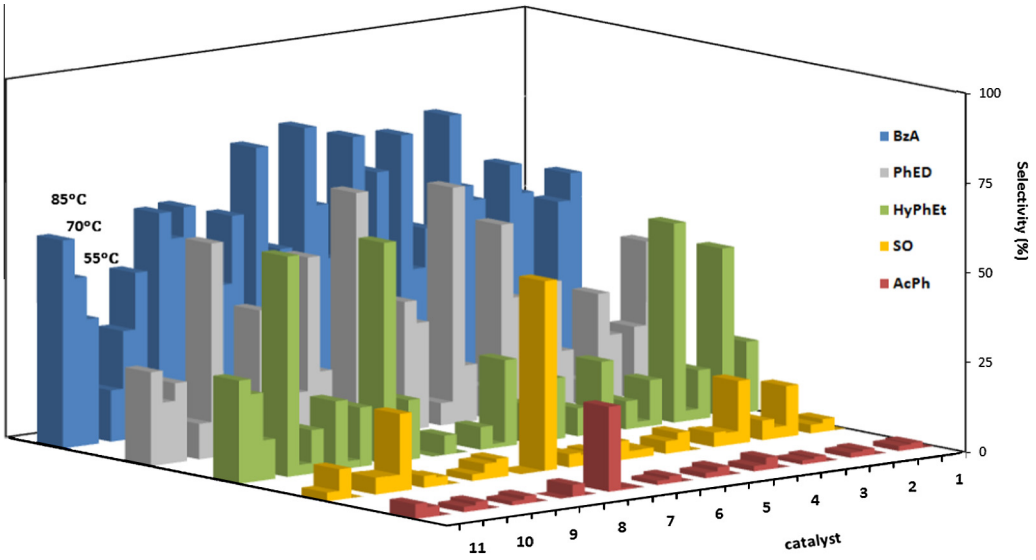

Fig. 10. Selectivity (%).[a] Effect of catalysts (**1**–**11**) on the oxidation of styrene at different temperatures (55, 70 y 85 °C), 15 h.[a] Reaction conditions: styrene (1.04 g,); catalyst (0.01 mmol); H_2O_2 (17.6 mmol); acetonitrile (10 mL).

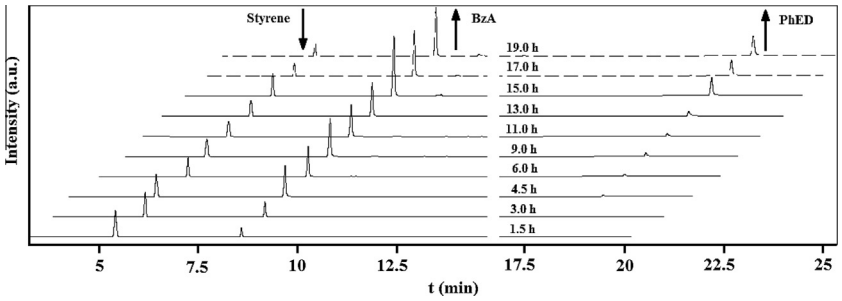

Fig. 11. Chromatograms of styrene oxidation with H_2O_2 using samarium complex (**9**) as catalysts at different reaction times.

influence of the ionic radius of the metal center of the complex in the catalytic process is not observed. Fig. 9(c) shows the effect of the temperature until 15 h for the Sm(III) complex (**9**). Increase in temperature is found to be favorable for styrene oxidation, so that, an increase of temperature led to much higher styrene conversion. For this catalyst, the influence of reaction time in the selectivity is discussed in Section 3.3.3.

3.3.3. Study of the influence of reaction time in the selectivity

The conversion and selectivity of styrene oxidation was monitored at different time periods until 19 h (at 70 °C) to evaluate the influence of reaction time in the catalytic activity of complex **9**. Fig. 11 shows the chromatograms of styrene oxidation with H_2O_2 in the presence of samarium complex **9** at different reaction times where is easily observed how the styrene concentration is decreasing with time (a decrease in the peak area is observed), while the concentration of BzA and PhED are increasing with time (an increase in the peak area is shown).

Fig. 12 shows the change in the conversion rate as well as the variation of the selectivity towards both of the main products of the reaction (BzA and PhED) with time. Initially, 20% styrene conversion and 98% BzA selectivity were obtained, a significant difference in the styrene conversion was subsequently observed when the reaction time was increased, reaching 89% conversion after 19 h, although with a decrease in the selectivity of BzA to 55%, offset by increased PhED selectivity that reached a selectivity of 40%. In general, the conversion of styrene is favored with increasing reaction time, but the selectivity is being affected.

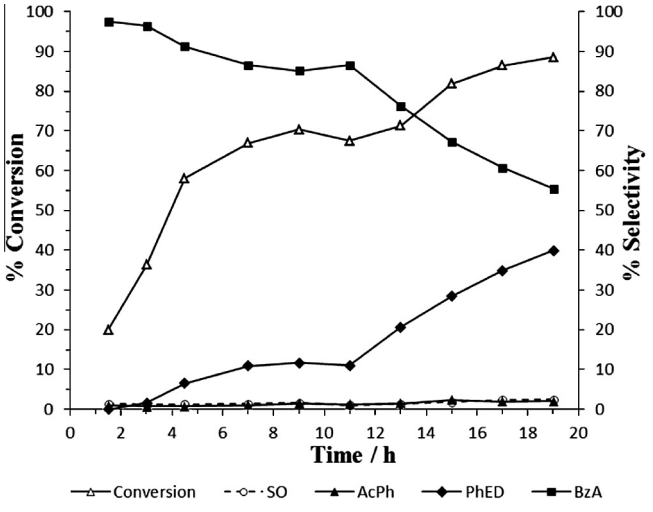

Fig. 12. Conversion of styrene and variation in the selectivity of different reaction products as a function of time using $[Sm(cinn)_3]\cdot H_2O$ (**9**) as catalyst.

Table 4
Effect of catalysts on the oxidation of styrene at different concentration of H_2O_2, catalyst concentration and reaction time, product selectivity and turn over number (TON).[a]

Catalyst	Catal:styrene	Time	Selectivity (%)					TON
		(h)	BzA	SO	AcPh	HyPhEt	PhED	
7	1:1000	2	81.25	0.90	0.00	6.20	10.88	628
		5	64.14	0.30	0.00	4.12	30.24	738
		8	31.59	0.00	0.00	12.13	56.28	756
		12	29.08	2.94	0.00	6.86	61.13	902
		15	28.06	0.00	0.00	6.26	65.03	995
	1:2000	2	71.04	1.29	0.00	5.36	19.88	1182
		5	64.89	1.51	0.33	4.83	27.02	1434
		8	28.42	2.42	0.00	11.38	57.77	1661
		12	46.59	0.00	0.00	13.33	16.71	1791
		15	22.94	0.00	0.00	16.86	58.35	1983
	1:4000	2	100.0	0.00	0.00	0.00	0.00	799
		5	67.68	0.00	0.00	0.00	32.32	789
		8	42.61	0.00	0.00	0.00	19.76	1547
		12	48.18	2.96	0.00	21.25	27.61	2770
		15	55.78	0.00	0.00	16.68	20.10	3779
	H_2O_2:styrene							
8	1:1	2	53.26	3.33	0.00	17.85	25.56	337
		5	53.18	2.42	0.00	15.16	29.24	458
		8	48.16	3.77	0.00	20.02	28.05	607
		12	45.13	4.48	1.78	23.33	21.54	657
		15	72.86	3.25	1.25	11.59	11.06	812
	2:1	2	58.02	1.99	0.00	10.05	26.42	313
		5	56.22	0.00	0.00	13.45	30.33	343
		8	55.39	3.48	0.94	11.05	23.67	466
		12	38.86	5.94	2.27	27.39	24.02	643
		15	45.94	4.63	1.87	17.14	21.76	690
	4:1	2	53.97	0.00	0.00	19.72	26.31	879
		5	70.93	0.78	0.00	12.58	13.45	909
		8	27.26	1.86	0.00	30.13	30.58	939
		12	25.92	2.00	0.48	51.87	16.99	959
		15	24.60	2.35	0.52	52.91	15.95	973

[a] Reaction conditions: styrene (500 mg); acetonitrile; 70 °C. Turn over number (TON): moles converted/moles of active site.

3.3.4. Study of the influence of the catalyst and oxidant concentration

The influence of H_2O_2:styrene and catalyst:styrene molar ratio on the conversion and selectivity has been studied and the results are presented in Fig. 9(d and e) and Table 4. In the effect of oxidant concentration, when the ratio is 4:1 (oxidant:substrate) from 2 h a high conversion rate (>85%) is observed, indicating that the peroxide has a great influence in this study. Before 15 h at 2:1 ratio (oxidant:substrate) the conversion is higher than 1:1, however, after 15 h, 1:1 ratio exceeds to 2:1 in conversion, notably improving the selectivity toward benzaldehyde. About the Oxidant effect one can also envisage that after 15 h of reaction, the peroxide concentration is directly proportional to the formation of HyPhEt and inversely proportional to BZA.

The influence of the concentration of catalyst is clearly seen when analyzing the results of Table 4. For the ratio 1:4000 (catalyst:substrate) a TON value of 3779 after 15 h is achieved, which is the highest value of all calculated. These results indicate that catalyst **7** is efficient even at very low concentrations. For the three concentrations tested, conversion ratio above 90% is obtained after 15 h. At shorter times, the conversion was always lower at 1:4000 ratio.

The selectivity toward products was moderately affected because at 1:4000 ratio the main product was BzA (56%), however, when using a higher concentration of catalyst the major product was PhED (55–65%).

4. Conclusions

A series of lanthanide complexes containing different cinnamate and phenylacetate ligands has been synthesized and characterized. The molecular structure of compound **11** has been determined. The toxicity of these compounds to macrophages and erythrocytes was tested observing non-toxicity in the studied range of concentrations which was up to 950 μM, indicating that these compounds can be considered as non-toxic for these primary cells. In view of the low toxicity showed by the compounds, the cytotoxicity effect in three different cancer cell lines was also assessed, observing, unfortunately, that the IC_{50} values of the lanthanide complexes were very high (between 542.7 ± 5.0 and >750 μM) which reflected a non-toxic activity against these cancer cell lines. This result indicated that these lanthanide compounds with cinnamate and/or phenylacetate ligands cannot be considered to be studied as potential anticancer agents. However, the catalytic studies on the styrene oxidation carried out for **1**–**11**, showed catalytic conversions of up to 99% with a selectivity towards PhED of ca. 70%. A detailed study of the catalytic reaction mixture at different time periods shows that the reaction conditions strongly affect the behavior of styrene oxidation reaction. Thus, an increase in the reaction time leads to a decrease of the selectivity towards BzA, indicating that reaction times longer than 19 h may lead to equimolar mixtures of BzA and PhED. Increase in temperature is found to be favorable for styrene oxidation. The selectivity to BzA and efficiency of H_2O_2 for oxidation of styrene could be raised by keeping a low concentration of hydrogen peroxide during short reaction times. Further investigations employing this type of catalyst in other reactions are currently in progress in our laboratory.

Acknowledgements

The authors are grateful to Colciencias, Universidad del Valle and the "Jóvenes Investigadores e Innovadores 2012" program for financial support to the master student. We would also like to thank financial support from the Ministerio de Economía y Competitividad, Spain (Grant No. CTQ2012-30762).

Appendix A. Supplementary data

CCDC 985957 contains the supplementary crystallographic data for **11**. These data can be obtained free of charge via http://www.ccdc.cam.ac.uk/conts/retrieving.html, or from the Cambridge Crystallographic Data Centre, 12 Union Road, Cambridge CB2 1EZ, UK; fax: (+44) 1223-336-033; or e-mail: deposit@ccdc.cam.ac.uk. Supplementary data associated with this article can be found, in the online version, at http://dx.doi.org/10.1016/j.poly.2014.02.040.

References

[1] S.H. van Rijt, P.J. Sadler, Drug Discovery Today 14 (2009) 1089.
[2] C. Saturnino, M. Bortoluzzi, M. Napoli, A. Popolo, A. Pinto, P. Longo, G. Paolucci, J. Pharm. Pharmacol. 65 (2013) 1354.
[3] N.S. Rukk, D.V. Albov, R.S. Shamsiev, S.N. Mudretsova, G.A. Davydova, G.G. Sadikov, A.S. Antsyshkina, V.V. Kravchenko, A.Y. Skryabina, G.N. Apryshko, V.V. Zamalyutin, E.A. Mironova, Polyhedron 44 (2012) 124.
[4] A. Hussain, S. Gadadhar, T.K. Goswami, A.A. Karande, A.R. Chakravarty, Eur. J. Med. Chem. 50 (2012) 319.
[5] Z.F. Chen, M.X. Tan, Y.C. Liu, Y. Peng, H.H. Wang, H.G. Liu, H. Liang, J. Inorg. Biochem. 105 (2011) 426.
[6] I. Kostova, G. Momekov, Appl. Organometal. Chem. 21 (2007) 226.
[7] E.L. Niero, G.M. Machado-Santelli, J. Exp. Clin. Cancer Res. 32 (2013) 31.
[8] C.M. Tsai, G.C. Yen, F.M. Sun, S.F. Yang, C.J. Weng, Mol. Pharm. 10 (2013) 1890.
[9] Z.H. Shi, N.G. Li, Q.P. Shi, Hao-Tang, Y.P. Tang, Drug Dev. Res. 73 (2012) 317.
[10] X.H. Yang, Q. Wen, T.T. Zhao, J. Sun, X. Li, M. Xing, X. Lu, H.L. Zhu, Med. Chem. 20 (2012) 1181.
[11] G.C. Yen, Y.L. Chen, F.M. Sun, Y.L. Chiang, S.H. Lu, C.J. Wenga, Eur. J. Pharm. Sci. 44 (2011) 281.
[12] Y. Qian, H.J. Zhang, H. Zhang, C. Xu, J. Zhao, H.L. Zhu, Med. Chem. 18 (2010) 4991.
[13] I. Aillaud, C. Olier, Y. Chapurina, J. Collin, E. Schulz, R. Guillot, J. Hannedouche, A. Trifonov, Organometallics 30 (2011) 3378.
[14] R. Sen, D. Saha, S. Koner, Catal. Lett. 142 (2012) 124.
[15] R. Sen, D.K. Hazra, M. Mukherjee, S. Koner, Eur. J. Inorg. Chem. (2011) 2826.
[16] R. Sen, D.K. Hazra, S. Koner, M. Helliwell, M. Mukherjee, A. Bhattacharjee, Polyhedron 29 (2010) 3183.
[17] T. Ohshima, T. Nemoto, S.Y. Tosaki, H. Kakei, V. Gnanadesikan, M. Shibasaki, Tetrahedron 59 (2003) 10485.
[18] E.T. Saka, İ. Acar, Z. Biyiklioğlu, H. Kantekin, İ. Kani, Synth. Met. 169 (2013) 12.
[19] G. Romanowski, J. Kira, Polyhedron 53 (2013) 172.
[20] V.R. Choudhary, D.K. Dumbre, N.S. Patil, B.S. Uphade, S.K. Bhargava, J. Catal. 300 (2013) 217.
[21] M.R. Maurya, M. Bisht, N. Chaudhary, F. Avecilla, U. Kumar, H.F. Hsu, Polyhedron 54 (2013) 180.
[22] C. Liu, J. Huang, D. Sun, Y. Zhou, X. Jing, M. Du, H. Wang, Q. Li, Appl. Catal. A: Gen. 459 (2013) 1.
[23] S. Gómez-Ruiz, G.N. Kaluđerović, S. Prashar, D. Polo-Cerón, M. Fajardo, Ž. Žižak, T.J. Sabo, Z.D. Juranić, J. Inorg. Biochem. 102 (2008) 1558.
[24] S. Gómez-Ruiz, G.N. Kaluđerović, S. Prashar, E. Hey-Hawkins, A. Erić, Ž. Žižak, Z.D. Juranić, J. Inorg. Biochem. 102 (2008) 2087.
[25] S. Gómez-Ruiz, S. Prashar, L.F. Sanchez-Barba, D. Polo-Cerón, M. Fajardo, A. Antiñolo, A. Otero, M.A. Maestro, C.J. Pastor, J. Mol. Catal. A. 264 (2007) 260.
[26] D. Polo-Cerón, S. Gómez-Ruiz, S. Prashar, M. Fajardo, A. Antiñolo, A. Otero, I. López-Solera, M.L. Reyes, J. Mol. Catal. A. 268 (2007) 264.
[27] G.B. Deacon, M. Forsyth, P.C. Junk, S.G. Leary, W.W. Lee, Z. Anorg. Allg. Chem. 635 (2009) 833.
[28] G.B. Deacon, C.M. Forsyth, P.C. Junk, M. Hilder, S.G. Leary, C. Bromant, I. Pantenburg, G. Meyer, B.W. Skelton, A.H. White, Z. Anorg. Allg. Chem. 634 (2008) 91.
[29] J. O'Brien, I. Wilson, T. Orton, F. Pognan, Eur. J. Biochem. 267 (2000) 5421.
[30] G.M. Sheldrick, SADABS, Program for area detector adsorption correction, Institute for Inorganic Chemistry, ,University of Göttingen, Germany, 1996.
[31] G.M. Sheldrick, SHELX-97, program for crystal structure refinement, University of Göttingen, Göttingen, Germany, 1997.
[32] M.A.S. Carvalho, N.S. Fernandes, F.L. Fertonani, M. Ionashiro, Thermochim. Acta 398 (2003) 93.
[33] T. Mihaylov, N. Trendafilova, I. Kostova, I. Georgieva, G. Bauer, Chem. Phys. 327 (2006) 209.
[34] G.B. Deacon, R.J. Philips, Coord. Chem. Rev. 33 (1980) 227.
[35] M.A.S. Carvalho, N.S. Fernandes, M.I.G. Leles, R. Mendes, M. Ionashiro, J. Therm. Anal. Calorim. 59 (2000) 669.
[36] A. Czylkowska, M. Markiewicz, J. Therm. Anal. Calorim. 109 (2012) 727.
[37] I. Kostova, Anti-Cancer Agents Med. Chem. 6 (2005) 591.